Nonlinear signal analysis used in GENESIS

Application to Herschel data

Genesis kick-off, 28-29 september 2017

H. Yahia, N. Schneider, S. Bontemps, G. Attuel

1 Geostat partner

Geostat

- **Geostat: Geometry & Statistics in acquisition data**. EPI INRIA BSO, `http://geostat.bordeaux.inria.fr/`
-
-
-

Geostat

- **Geostat: Geometry & Statistics in acquisition data**. EPI INRIA BSO, `http://geostat.bordeaux.inria.fr/`
- INRIA research team specialized in the analysis of complex natural signals and time series.
-
-

Geostat

- **Geostat: Geometry & Statistics in acquisition data**. EPI INRIA BSO, `http://geostat.bordeaux.inria.fr/`
- INRIA research team specialized in the analysis of complex natural signals and time series.
- Strong collaboration with CNRS LEGOS (Toulouse) on analysis of oceanic data from remote sensing.
-

Geostat

- **Geostat: Geometry & Statistics in acquisition data**. EPI INRIA BSO, `http://geostat.bordeaux.inria.fr/`
- INRIA research team specialized in the analysis of complex natural signals and time series.
- Strong collaboration with CNRS LEGOS (Toulouse) on analysis of oceanic data from remote sensing.
- 3 full time researchers (Yahia, Daoudi, Brodu), 1 associate researcher (Attuel) plus post-docs and PhD students.

Analysis of turbulent signals

Analysis of turbulent signals

- Usual linear approaches based on Fourier not effective.
-
-

Analysis of turbulent signals

- Usual linear approaches based on Fourier not effective.
- Make use of advanced (time-frequency, wavelets, multifractal) methods to extract the dynamics characteristics of turbulence:

.

-

Analysis of turbulent signals

- Usual linear approaches based on Fourier not effective.
- Make use of advanced (time-frequency, wavelets, multifractal) methods to extract the dynamics characteristics of turbulence: **multiplicative cascades**.
-

Analysis of turbulent signals

- Usual linear approaches based on Fourier not effective.
- Make use of advanced (time-frequency, wavelets, multifractal) methods to extract the dynamics characteristics of turbulence: **multiplicative cascades**.
- **Coupling physics/signal processing to analyze Herschel data.**

2
Analysis of turbulent data

K41

- Phenomelogical description of HDT (*i.e.* still non-proved today from Navier-Stokes equations), Kolmogorov descrioption, fllowed by Parisi-Frish & She-Levêque.
-

K41

- Phenomelogical description of HDT (*i.e.* still non-proved today from Navier-Stokes equations), Kolmogorov descrioption, fllowed by Parisi-Frish & She-Levêque.
- NS equation in incompressible HD case:

$$\partial_t \mathbf{v} + \mathbf{v} \cdot \nabla \mathbf{v} = -\nabla p + \nu \nabla^2 \mathbf{v}$$
$$\nabla \cdot \mathbf{v} = 0.$$

plus limit conditions, ν: kinematic viscosity coefficient.

K41

- At Reynolds $R = \dfrac{LV}{\nu} \to \infty$, symmétries (coming from discrete or continuous groups preserving solutions of NS equations) are restored in a statistical sense only: **fully developed turbulence**.

K41

- Let $\varepsilon_r(\mathbf{x})$ be the local energy dissipation at point $\mathbf{x}$ in a ball $\mathcal{B}_r(\mathbf{x})$ of radius r centered at $\mathbf{x}$:

$$\varepsilon_r(\mathbf{x}) = \frac{1}{\lambda(\mathcal{B}_r(\mathbf{x}))} \int_{\mathcal{B}_r(\mathbf{x})} \sum_{i,j} (\partial_i \mathbf{v}_j(\mathbf{y}) + \partial_j \mathbf{v}_i(\mathbf{y}))^2 \mathrm{d}\mathbf{y} \qquad (1)$$

-
-

K41

- Let $\varepsilon_r(\mathbf{x})$ be the local energy dissipation at point $\mathbf{x}$ in a ball $\mathcal{B}_r(\mathbf{x})$ of radius r centered at $\mathbf{x}$:

$$\varepsilon_r(\mathbf{x}) = \frac{1}{\lambda(\mathcal{B}_r(\mathbf{x}))} \int_{\mathcal{B}_r(\mathbf{x})} \sum_{i,j} (\partial_i \mathbf{v}_j(\mathbf{y}) + \partial_j \mathbf{v}_i(\mathbf{y}))^2 \mathrm{d}\mathbf{y} \qquad (3)$$

- for each scale r, (ε_r) is a stochastic process indexed by $\mathbf{x}$.
-

K41

- Let $\varepsilon_r(\mathbf{x})$ be the local energy dissipation at point $\mathbf{x}$ in a ball $\mathcal{B}_r(\mathbf{x})$ of radius r centered at $\mathbf{x}$:

$$\varepsilon_r(\mathbf{x}) = \frac{1}{\lambda(\mathcal{B}_r(\mathbf{x}))} \int_{\mathcal{B}_r(\mathbf{x})} \sum_{i,j} (\partial_i \mathbf{v}_j(\mathbf{y}) + \partial_j \mathbf{v}_i(\mathbf{y}))^2 \mathrm{d}\mathbf{y} \qquad (5)$$

- for each scale r, (ε_r) is a stochastic process indexed by $\mathbf{x}$.
- Kolmogorov: for two scales $r < l$, in law:

$$\mathrm{d}\mathbb{P}_{\varepsilon_r} = \mathrm{d}\mathbb{P}_{\eta_{rl}} \mathrm{d}\mathbb{P}_{\varepsilon_l} \qquad (6)$$

η_{rl}: injection process between scales available within an **inertial range** $[r_1, r_2]$.

K41

- Original Kolmogorov hypothesis: η_{rl} is a constant $= (\frac{r}{l})^{-\alpha}$ leading to implications on the moments:

$$\langle \varepsilon_r^p \rangle = \left(\frac{r}{l}\right)^{-\alpha p} \langle \varepsilon_l^p \rangle \sim r^{-\alpha p} \tag{7}$$

-
-
-

K41

- Original Kolmogorov hypothesis: η_{rl} is a constant $= (\frac{r}{l})^{-\alpha}$ leading to implications on the moments:

$$\langle \varepsilon_r^p \rangle = \left(\frac{r}{l}\right)^{-\alpha p} \langle \varepsilon_l^p \rangle \sim r^{-\alpha p} \tag{8}$$

- Self-similarity: $\langle \varepsilon_r^p \rangle \sim r^{\tau_p}$, confirmed by experiments but
-
-

K41

- Original Kolmogorov hypothesis: η_{rl} is a constant $= (\frac{r}{l})^{-\alpha}$ leading to implications on the moments:

$$\langle \varepsilon_r^p \rangle = \left(\frac{r}{l}\right)^{-\alpha p} \langle \varepsilon_l^p \rangle \sim r^{-\alpha p} \tag{9}$$

- Self-similarity: $\langle \varepsilon_r^p \rangle \sim r^{\tau_p}$, confirmed by experiments but
- actually τ_p is not a linear function of p, instead a concave function of p: **anomalous scaling** .
-

K41

- Original Kolmogorov hypothesis: η_{rl} is a constant $= (\frac{r}{l})^{-\alpha}$ leading to implications on the moments:

$$\langle \varepsilon_r^p \rangle = \left(\frac{r}{l}\right)^{-\alpha p} \langle \varepsilon_l^p \rangle \sim r^{-\alpha p} \tag{10}$$

- Self-similarity: $\langle \varepsilon_r^p \rangle \sim r^{\tau_p}$, confirmed by experiments but
- actually τ_p is not a linear function of p, instead a concave function of p: **anomalous scaling** .
- η_{rl} must be replaced by a stochastic process independent of ε_l and **indefinitely divisible: multiplicative cascade**.

Parisi-Frisch

- Parisi-Frisch generalization: local scale laws:

$$\varepsilon_r(\mathbf{x}) \sim r^{\mathbf{h}(\mathbf{x})} \tag{11}$$

-
-
-

Parisi-Frisch

- Parisi-Frisch generalization: local scale laws:

$$\varepsilon_r(\mathbf{x}) \sim r^{\mathbf{h}(\mathbf{x})} \tag{13}$$

- $\mathbf{h}(\mathbf{x})$: singularity exponent at $\mathbf{x}$. Difficult to compute with precision.
-
-

Parisi-Frisch

- Parisi-Frisch generalization: local scale laws:

$$\varepsilon_r(\mathbf{x}) \sim r^{\mathbf{h}(\mathbf{x})} \tag{15}$$

- $\mathbf{h}(\mathbf{x})$: singularity exponent at $\mathbf{x}$. Difficult to compute with precision.
- Lead to a multifractal hierarchy: $\mathcal{F}_h = \{\mathbf{x} \mid \mathbf{h}(\mathbf{x}) = \mathbf{h}\}$ and

$$\mathrm{MSM} = \mathcal{F}_\infty = \{\mathbf{x} \mid \mathbf{h}(\mathbf{x}) \in]h_\infty - \Delta h, h_\infty + \Delta h[\}. \tag{16}$$

-

Parisi-Frisch

- Parisi-Frisch generalization: local scale laws:

$$\varepsilon_r(\mathbf{x}) \sim r^{\mathbf{h}(\mathbf{x})} \tag{17}$$

- $\mathbf{h}(\mathbf{x})$: singularity exponent at $\mathbf{x}$. Difficult to compute with precision.
- Lead to a multifractal hierarchy: $\mathcal{F}_h = \{\mathbf{x} \mid \mathbf{h}(\mathbf{x}) = \mathbf{h}\}$ and

$$\mathrm{MSM} = \mathcal{F}_\infty = \{\mathbf{x} \mid \mathbf{h}(\mathbf{x}) \in]h_\infty - \Delta h, h_\infty + \Delta h[\}. \tag{18}$$

- The **singularity spectrum** is $\mathbf{h} \to \dim(\mathcal{F}_h)$

Parisi-Frisch

- The τ_p and $\mathbf{h} \to D(\mathbf{h})$ are related by a Legendre Transform:

$$\tau_p = \inf_{\mathbf{h}} \{\mathbf{h}p + d - D(\mathbf{h})\}. \tag{19}$$

-
-
-

Parisi-Frisch

- The τ_p and $\mathbf{h} \rightarrow D(\mathbf{h})$ are related by a Legendre Transform:

$$\tau_p = \inf_{\mathbf{h}} \{\mathbf{h}p + d - D(\mathbf{h})\}. \tag{21}$$

- Thermodynamics analogy: τ_p free energy, $\mathbf{h} \rightarrow$ internal energy per volume unit and $D(\mathbf{h}) \rightarrow$ entropy.
-
-

Parisi-Frisch

- The τ_p and $\mathbf{h} \to D(\mathbf{h})$ are related by a Legendre Transform:

$$\tau_p = \inf_{\mathbf{h}} \{\mathbf{h}p + d - D(\mathbf{h})\}. \tag{23}$$

- Thermodynamics analogy: τ_p free energy, $\mathbf{h} \to$ internal energy per volume unit and $D(\mathbf{h}) \to$ entropy.
- $\tau_p = \inf_{\mathbf{h}} \{\mathbf{h}p + d - D(\mathbf{h})\}$ relates statistical properties to geometry. Knowledge of the singularity spectrum provides information on the underlying cascade processes.
-

Parisi-Frisch

- The τ_p and $\mathbf{h} \to D(\mathbf{h})$ are related by a Legendre Transform:

$$\tau_p = \inf_{\mathbf{h}} \{\mathbf{h}p + d - D(\mathbf{h})\}. \tag{25}$$

- Thermodynamics analogy: τ_p free energy, $\mathbf{h} \to$ internal energy per volume unit and $D(\mathbf{h}) \to$ entropy.
- $\tau_p = \inf_{\mathbf{h}}\{\mathbf{h}p + d - D(\mathbf{h})\}$ relates statistical properties to geometry. Knowledge of the singularity spectrum provides information on the underlying cascade processes.
- For a large class of complex systems, the following duality on Legendre spectrum is observed:

$$D(\mathbf{h}) = \inf_{\mathbf{h}} \{\mathbf{h}p + d - \tau_p\}. \tag{26}$$

3
Examples

"Easy case": observer on top

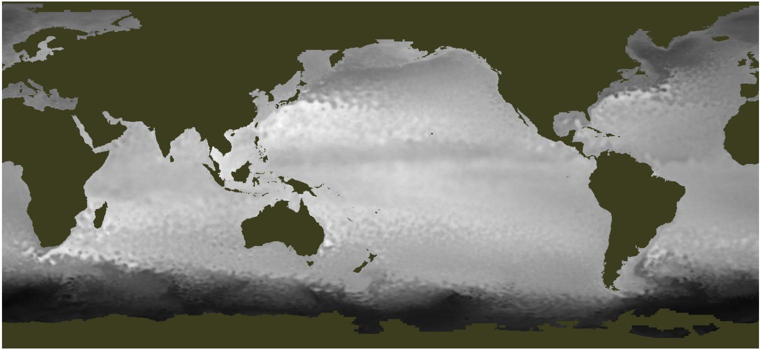

Figure: Oceanic data: altimetry and meso-scale turbulence.

"Easy case": observer on top

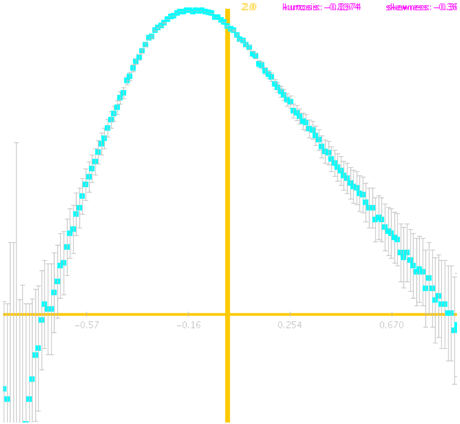

Figure: Oceanic data: altimetry and meso-scale turbulence. Area 1.

"Easy case": observer on top

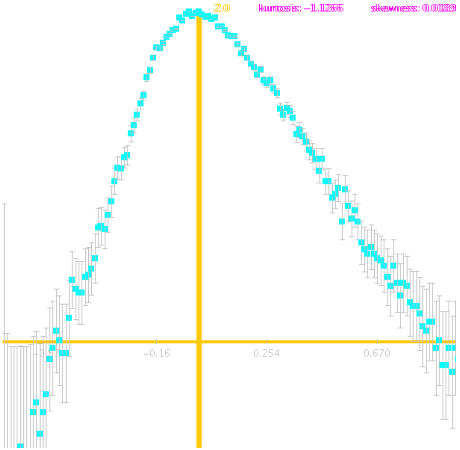

Figure: Oceanic data: altimetry and meso-scale turbulence. Area 2 (East of japan).

Draco

The *Draco* cloud: a high-velocity, translucent and diffuse cloud

- infalling gas from the halo or
- swept-up gas from shocks (SN explosions)
- local CO and CH detections (Stark et al. 1997, Meybold et al. 1985)

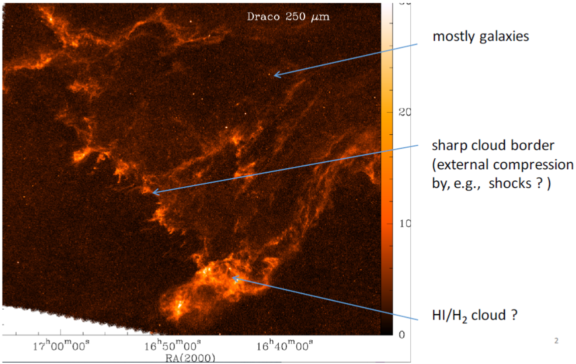

Figure: Courtesy N. Schneider.

Draco

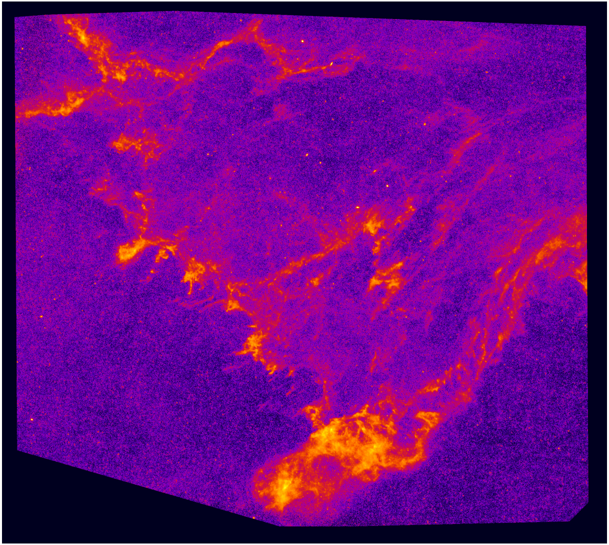

Draco singularity exponents

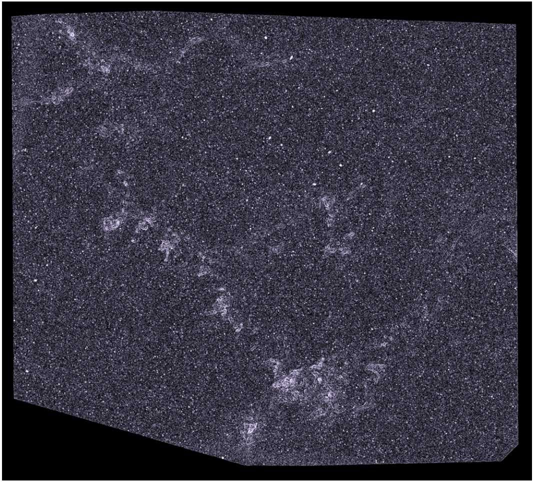

Draco singularity exponents

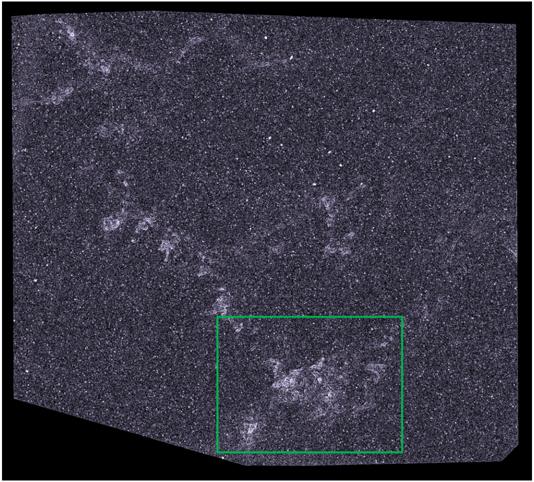

Figure: sub-region

Draco singularity exponents

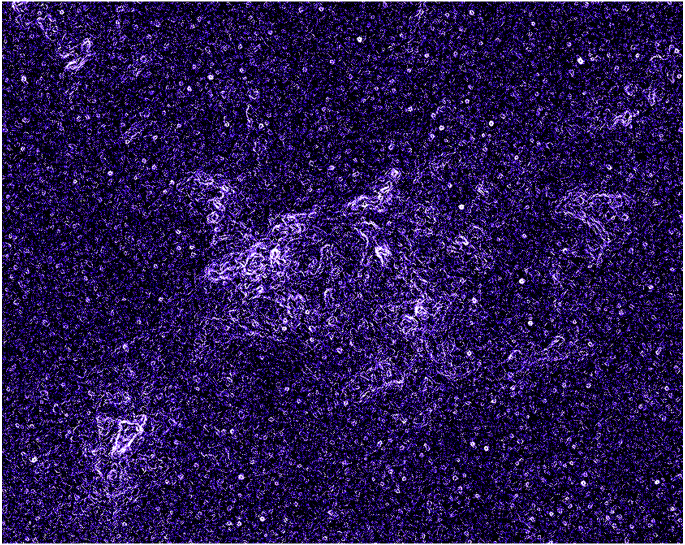

Draco singularity spectrum

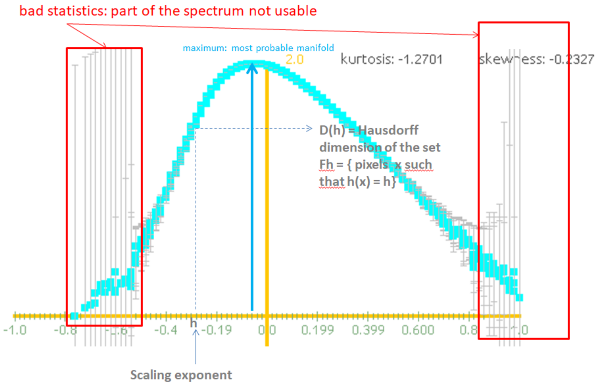

Figure: Draco spectrum

Draco psw sub-region 1

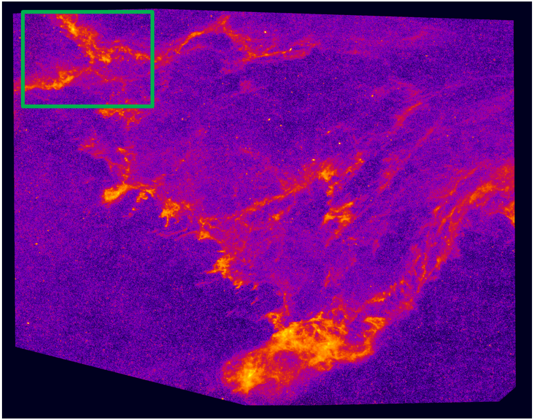

Figure: sub-region 1

Draco psw sub-region 1

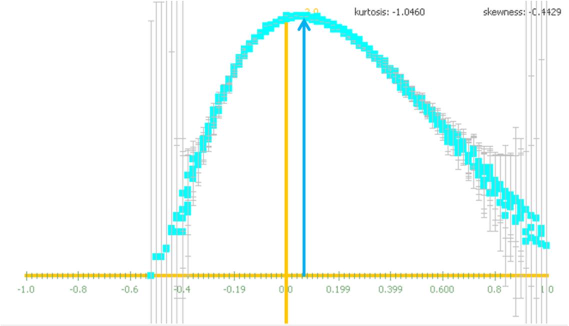

Draco psw sub-region 2

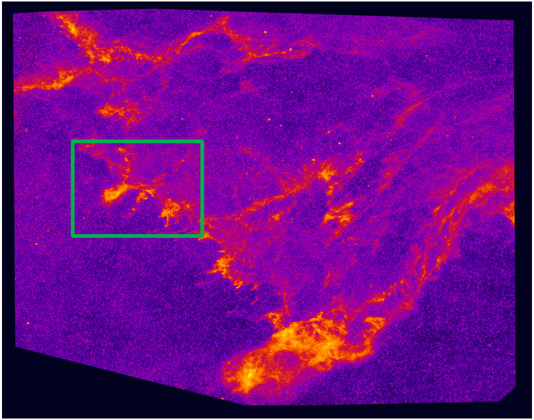

Figure: sub-region 2

Draco psw sub-region 2

Same most probable manifold as sub-region 1.

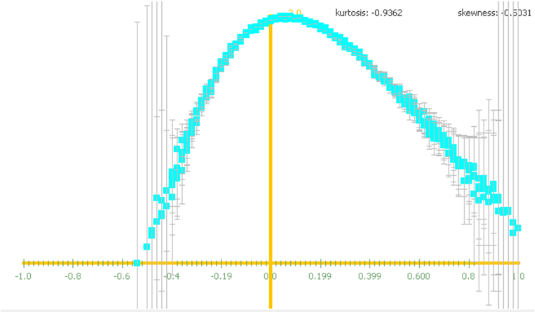

Draco psw sub-region 3

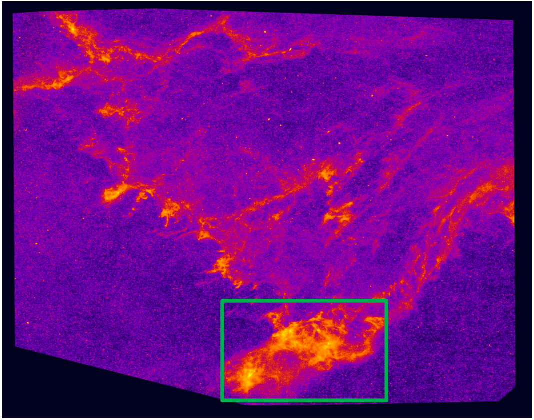

Figure: sub-region 3

Draco psw sub-region 3

Same most probable manifold as sub-regions 1 and 2. Same spectrum.

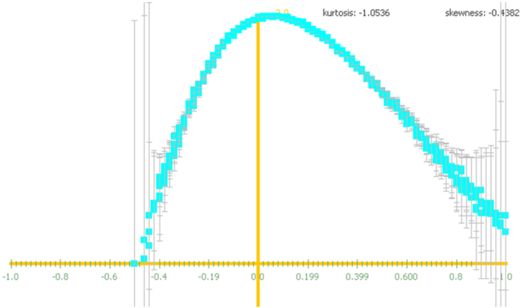

Draco psw sub-region 4

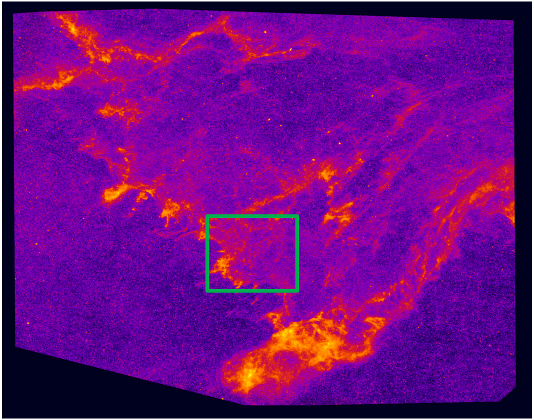

Figure: sub-region 4

Draco psw sub-region 4

Same most probable manifold as sub-regions 1, 2 and 3. Same spectrum.

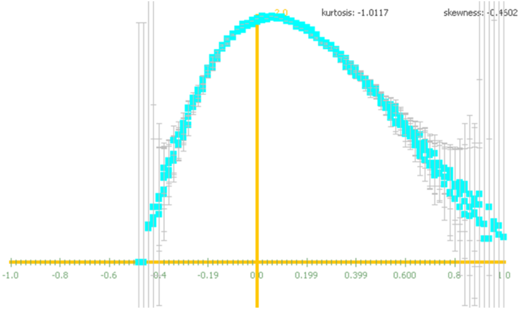

Draco psw sub-region 5

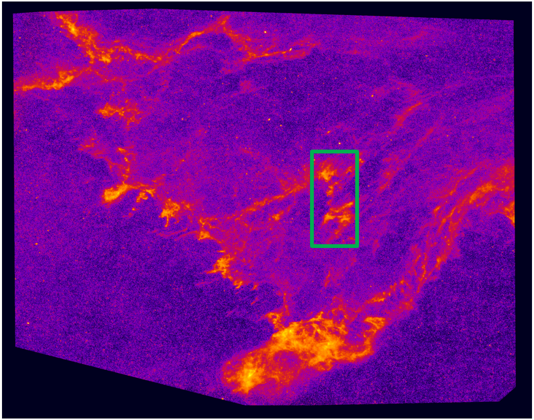

Figure: sub-region 5

Draco psw sub-region 5

Same most probable manifold as sub-regions 1, 2, 3 and 4. Same spectrum.

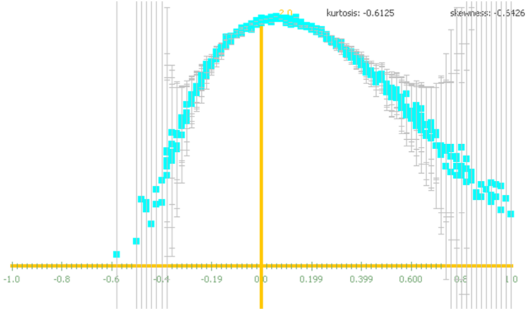

Draco psw sub-region 6

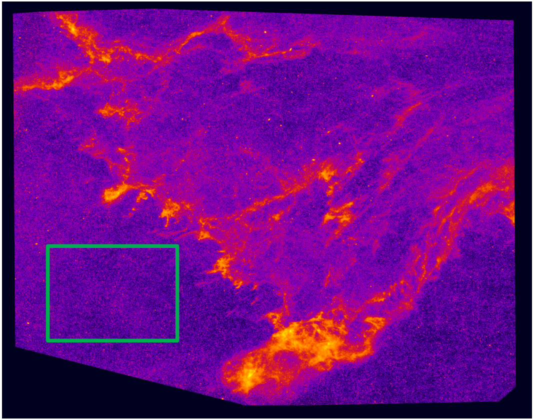

Figure: sub-region 6

Draco psw sub-region 6

Same most probable manifold as sub-regions 1, 2, 3, 4 and 5. Same spectrum.

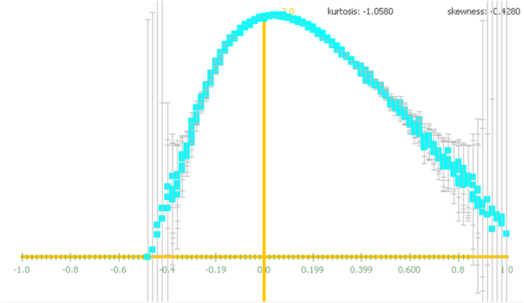

Draco sub-regions

- No differences in spectra.
- Different and much more difficult situation than in remote sensing data.
- Full 3D turbulence acquired along the line of sight: we observe a fully 3D turbulent cloud.
- We cannot "elementary partition" sub-regions to isolate specific behaviours: 3D mixing everywhere, same apparent spectra.

Consistency wrt wavelength acquisitions

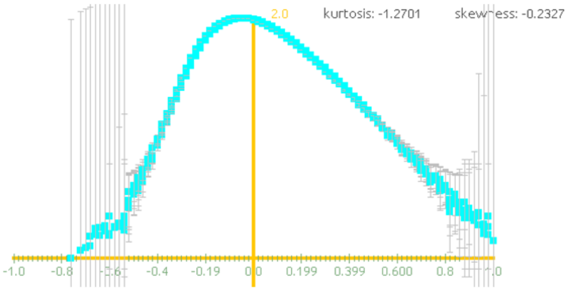

Figure: psw

Consistency wrt wavelength acquisitions

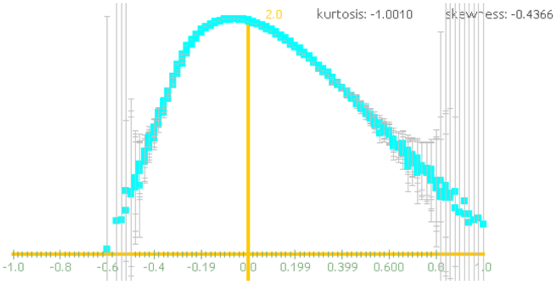

Figure: plw

Consistency wrt wavelength acquisitions

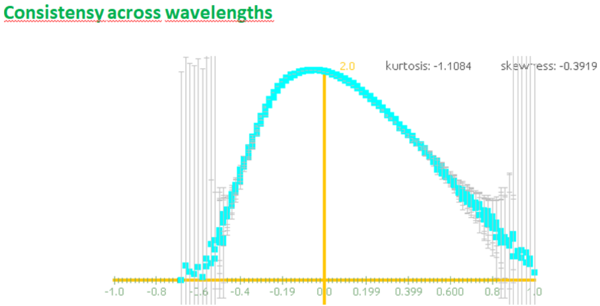

Figure: pmw

Manifolds $\mathcal{F}_h$

-
-
-

Manifolds $\mathcal{F}_h$

- $\mathcal{F}_h = \{\mathbf{x} \mid \mathbf{h}(\mathbf{x}) \in]\mathbf{h} - \Delta, \mathbf{h} + \Delta[\}$.
-
-

Manifolds $\mathcal{F}_h$

- $\mathcal{F}_h = \{\mathbf{x} \mid \mathbf{h}(\mathbf{x}) \in]\mathbf{h} - \Delta, \mathbf{h} + \Delta[\}$.
- In the following experiments, we take $\Delta = 0.08$.
-

Manifolds $\mathcal{F}_h$

- $\mathcal{F}_h = \{\mathbf{x} \mid \mathbf{h}(\mathbf{x}) \in]\mathbf{h}-, \mathbf{h} + \Delta[\}$.
- In the following experiments, we take $\Delta = 0.08$.
- Spectrum recomputed over $\mathcal{F}_h$ from original data.

Manifolds $\mathcal{F}_h$

-
-

Manifolds $\mathcal{F}_h$

- For $\Delta \to 0$ the spectrum converges weakly to a Dirac at h.
-

Manifolds $\mathcal{F}_h$

- For $\Delta \to 0$ the spectrum converges weakly to a Dirac at h.
- However we observe phenomena at amplitude cuts.

$\mathcal{F}_{-0.3}$

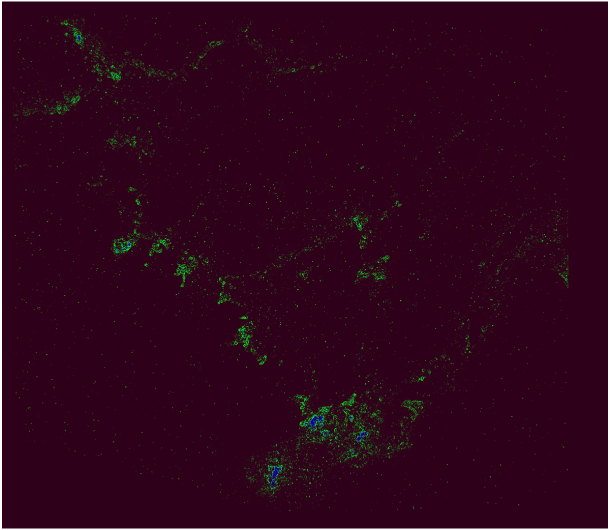

Figure: $\mathcal{F}_{-0.3}$

$\mathcal{F}_{-0.1}$

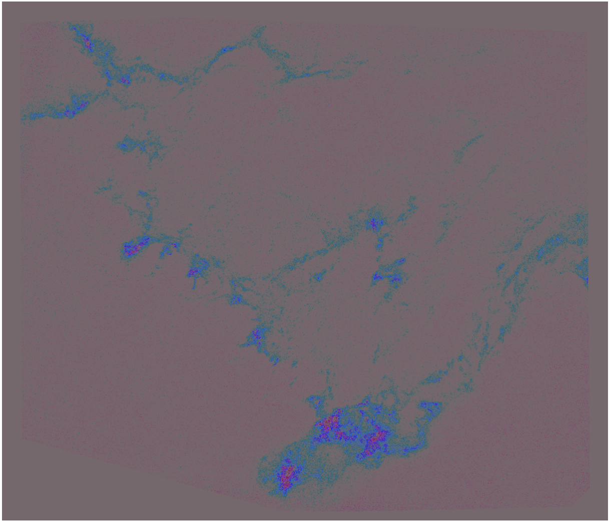

Figure: $\mathcal{F}_{-0.1}$

$\mathcal{F}_0$

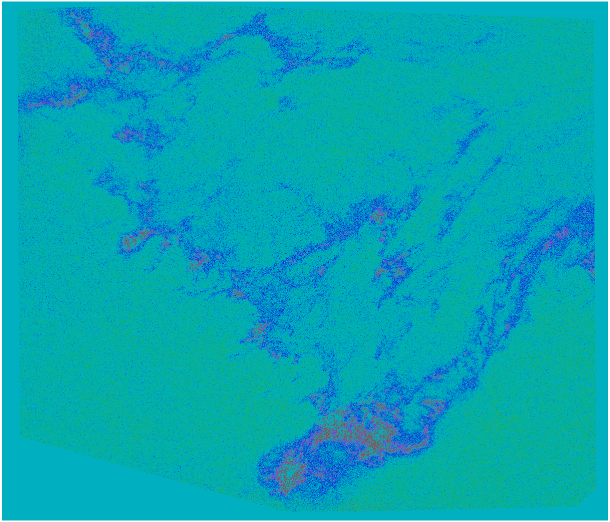

Figure: $\mathcal{F}_0$

Spectrum $\mathcal{F}_{-0.3}$

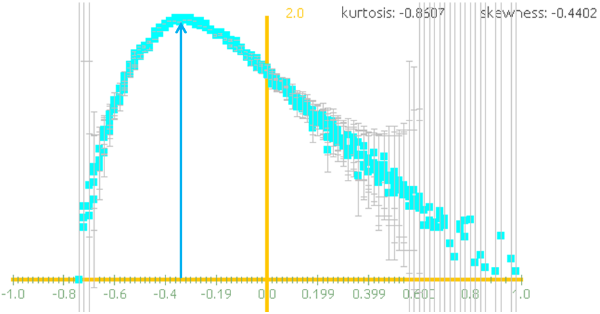

Spectrum $\mathcal{F}_{-0.3}$, cut at 0.5 in the data

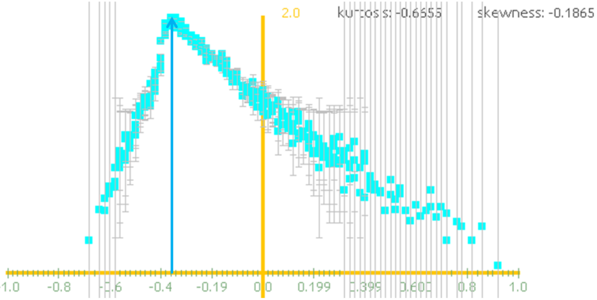

Spectrum $\mathcal{F}_{-0.3}$, cut at 1.5 in the data

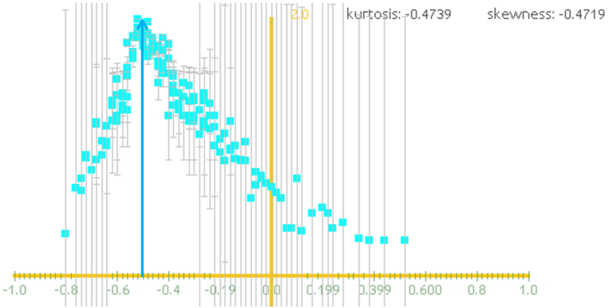

Spectrum $\mathcal{F}_{-0.15}$

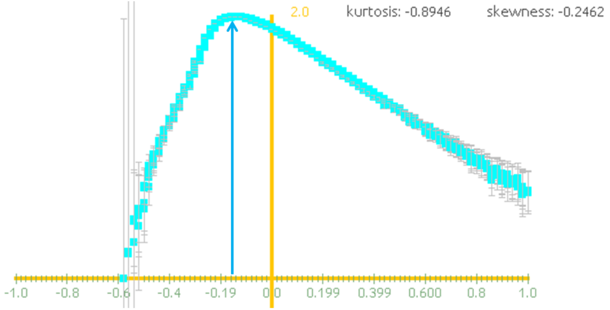

Spectrum $\mathcal{F}_{-0.16}$

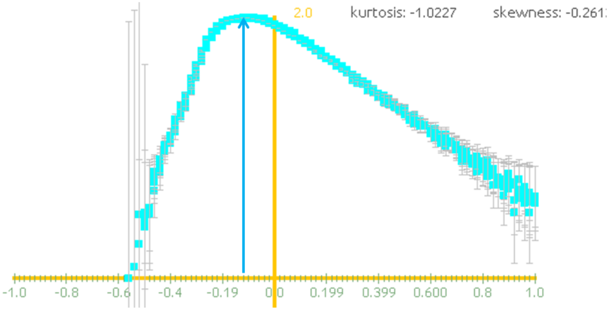

Spectrum $\mathcal{F}_0$

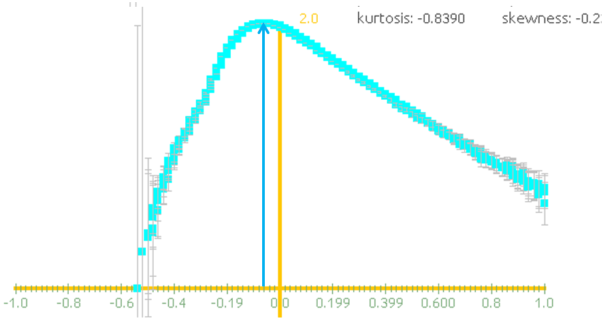

Manifolds $\mathcal{F}_h$

- Interpret the amplitude cut vs monofractal noise ?
-

Manifolds $\mathcal{F}_h$

- Interpret the amplitude cut vs monofractal noise ?
- The cut corresponds more or less to background. Role of background ?

Manifolds $\mathcal{G}_h$

Manifolds $\mathcal{G}_h$

- $\mathcal{G}_h = \{\mathbf{x} \mid \mathbf{h}(\mathbf{x}) \in]\mathbf{h}_\infty, \mathbf{h}[\}$.
-
-
-

Manifolds $\mathcal{G}_h$

- $\mathcal{G}_h = \{\mathbf{x} \mid \mathbf{h}(\mathbf{x}) \in]\mathbf{h}_\infty, \mathbf{h}[\}$.
- Spectrum is recomputed over $\mathcal{G}_h$ from the original data.
-
-

Manifolds $\mathcal{G}_h$

- $\mathcal{G}_h = \{\mathbf{x} \mid \mathbf{h}(\mathbf{x}) \in]\mathbf{h}_\infty, \mathbf{h}[\}$.
- Spectrum is recomputed over $\mathcal{G}_h$ from the original data.
- Over $\mathcal{G}_h$ the spectrum needs not to be close to a Dirac.
-

Manifolds $\mathcal{G}_h$

- $\mathcal{G}_h = \{\mathbf{x} \mid \mathbf{h}(\mathbf{x}) \in]\mathbf{h}_\infty, \mathbf{h}[\}$.
- Spectrum is recomputed over $\mathcal{G}_h$ from the original data.
- Over $\mathcal{G}_h$ the spectrum needs not to be close to a Dirac.
- These manifolds are probably more interesting candidates to study turbulence.

Manifold $\mathcal{G}_{-0.12}$

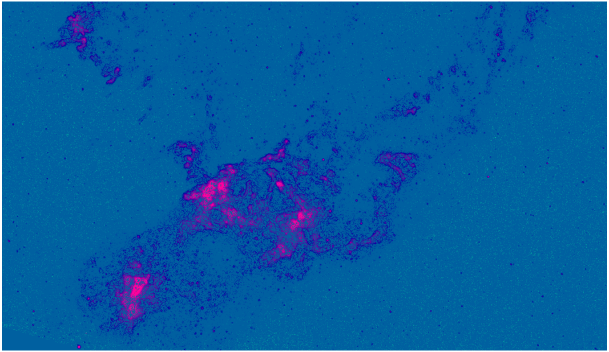

Spectrum $\mathcal{G}_{-0.4}$

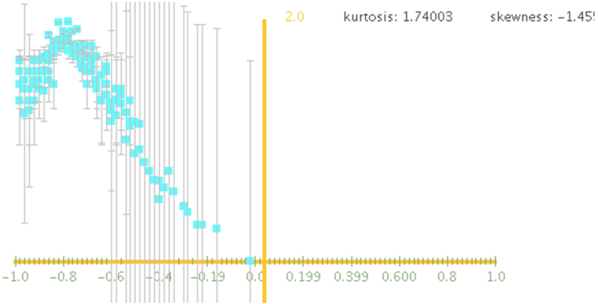

Spectrum $\mathcal{G}_{-0.36}$

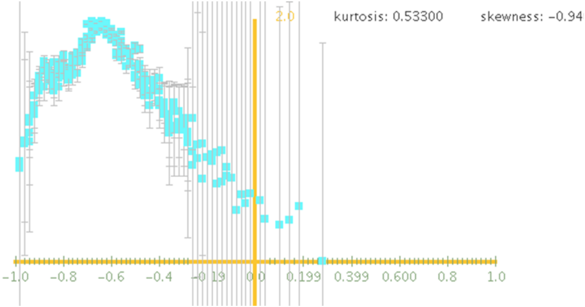

Spectrum $\mathcal{G}_{-0.31}$

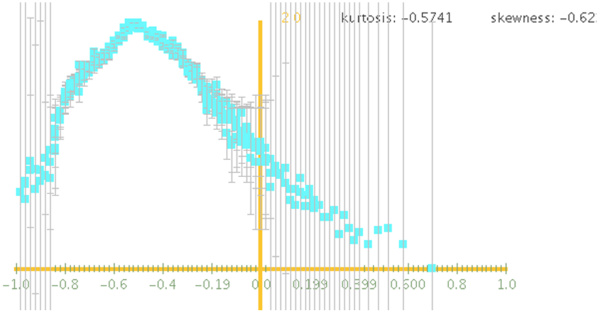

Spectrum $\mathcal{G}_{-0.27}$

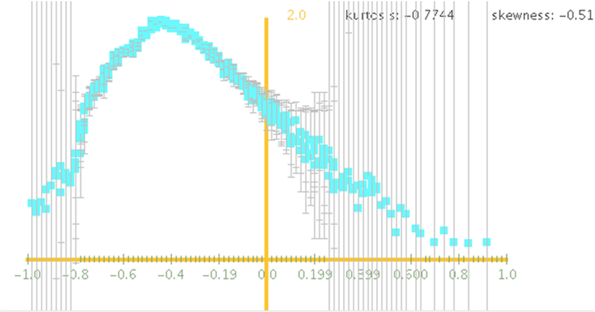

Spectrum $\mathcal{G}_{-0.23}$

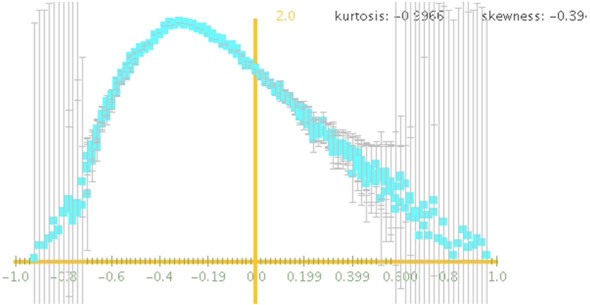

Spectrum $\mathcal{G}_{-0.2}$

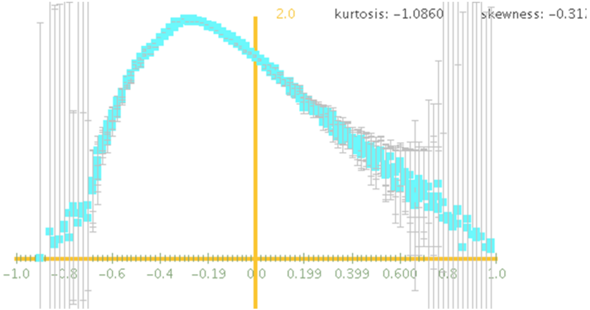

Spectrum $\mathcal{G}_{-0.16}$

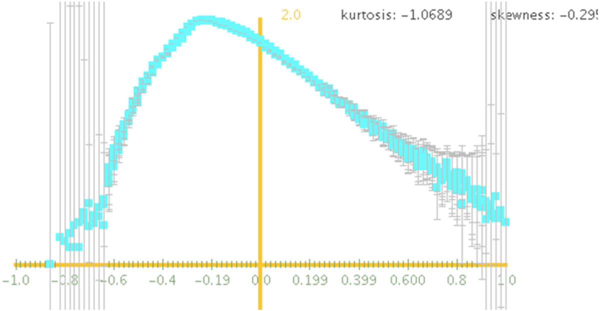

Spectrum $\mathcal{G}_{-0.1}$

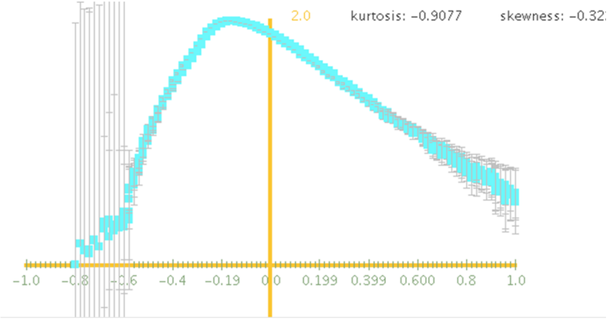

Spectrum $\mathcal{G}_{-0.1}$, cut at 0.5 in the data

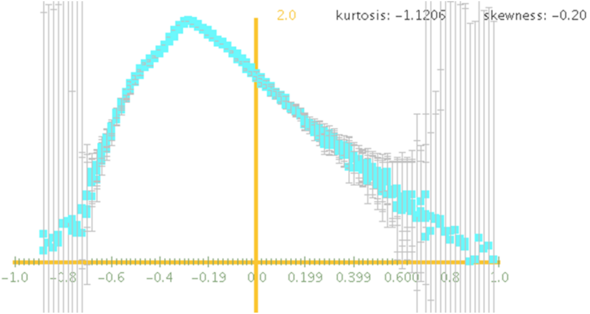

Spectrum $\mathcal{G}_0$

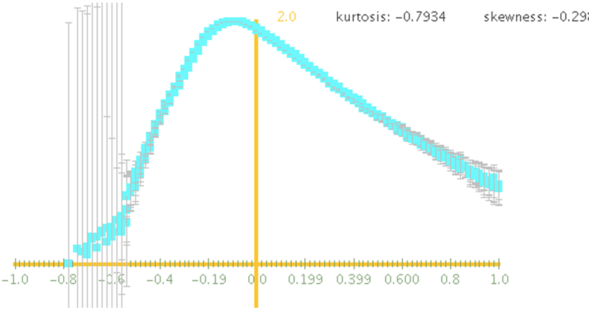

Lena

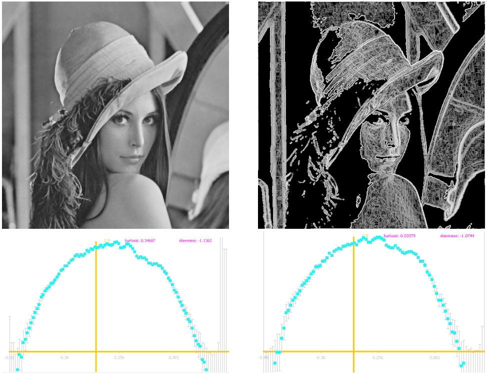

Figure: Lena.

Musca

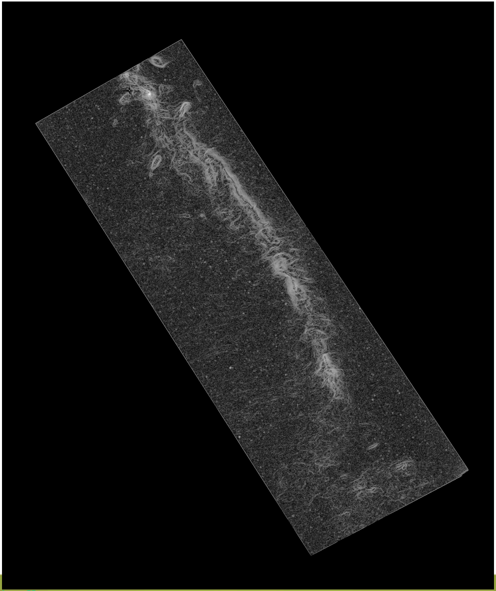

Musca

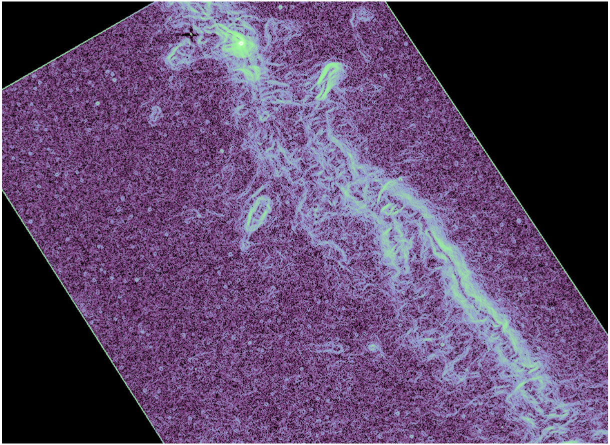

Figure: Musca SEs, zoom.

Musca

- As for Draco, no simple partitioning into regions of different spectra.
- **But we notice differences in the left part of some sub-regions spectra**.
- **The left part is the most informative part of the spectrum**.

Musca

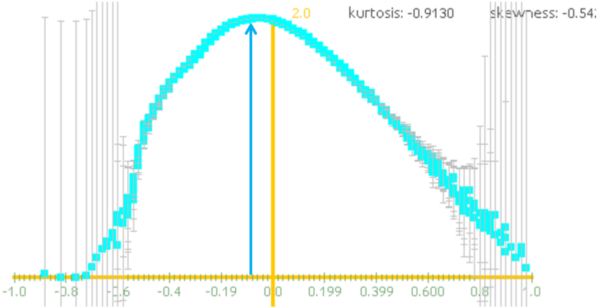

Figure: Musca spectrum.

Musca subregion

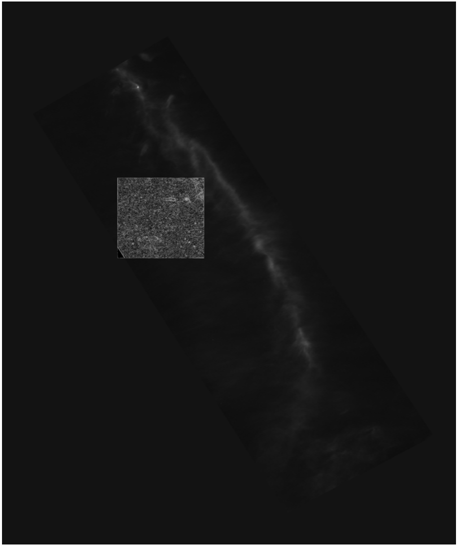

Figure: Musca subregion 3.

Musca subregion

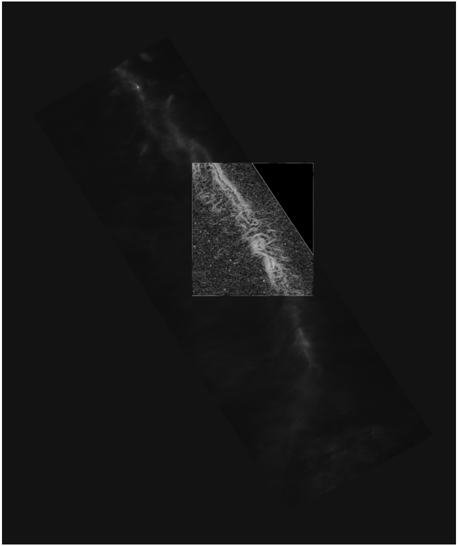

Figure: Musca subregion 5.

Musca subregion

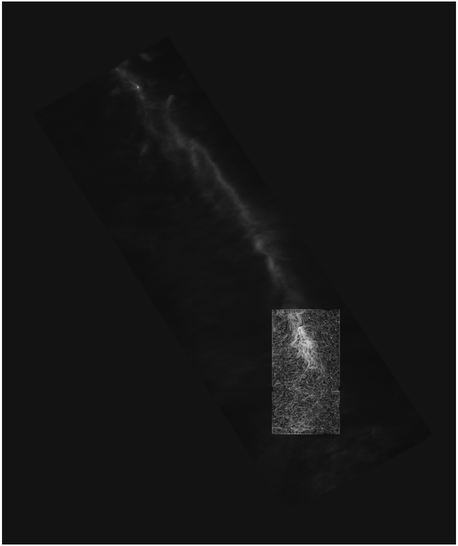

Figure: Musca subregion 6.

Musca subregion

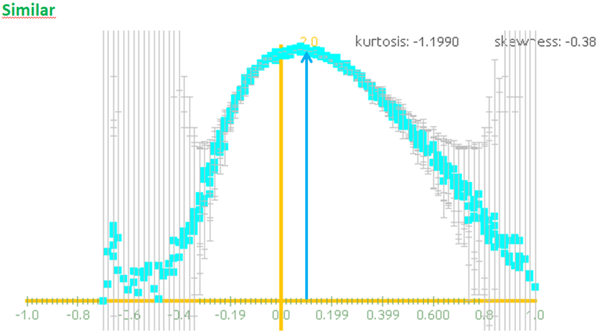

Figure: Musca subregion 3 spectrum.

Musca subregion

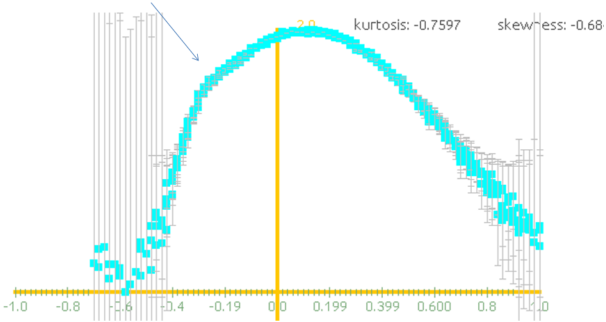

Figure: Musca subregion 5 spectrum.

Musca subregion

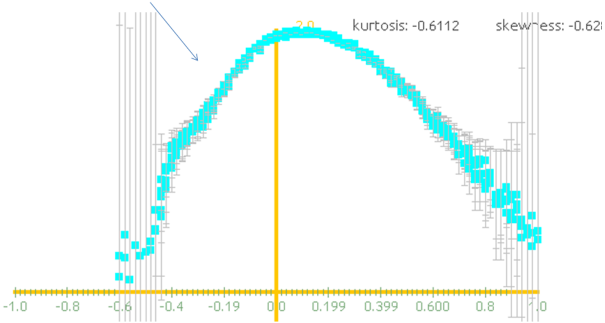

Figure: Musca subregion 6 spectrum.

Musca $\mathcal{F}_{-0.4}$

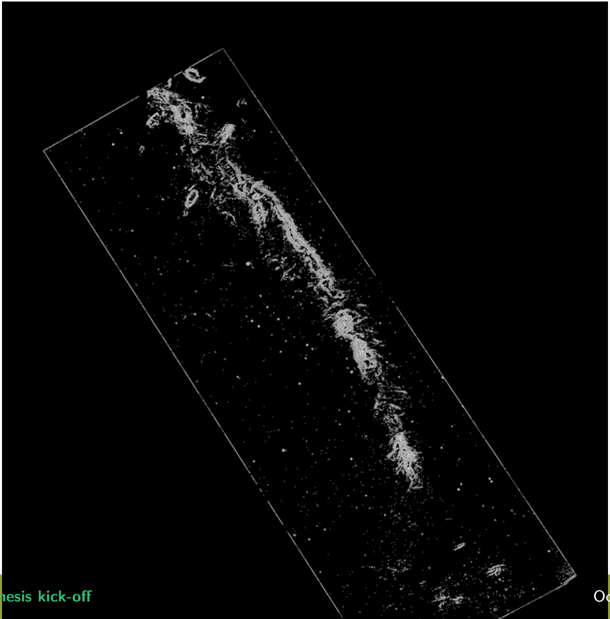

Musca $\mathcal{F}_{-0.2}$

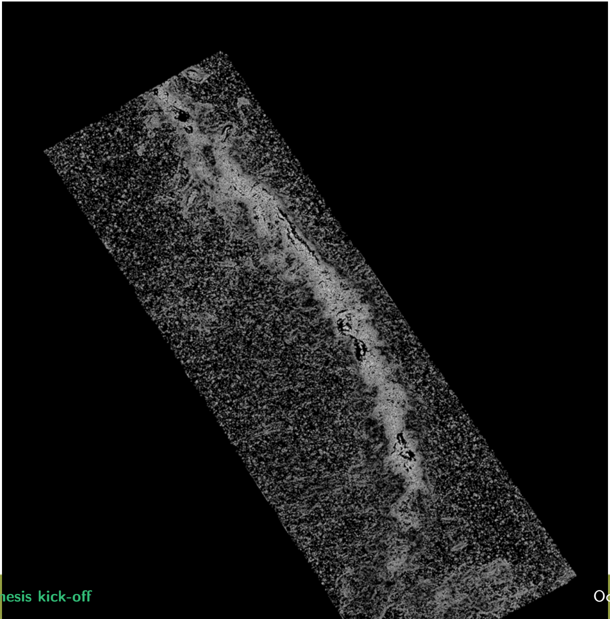

Musca $\mathcal{F}_{-0.2}$ cut at 0

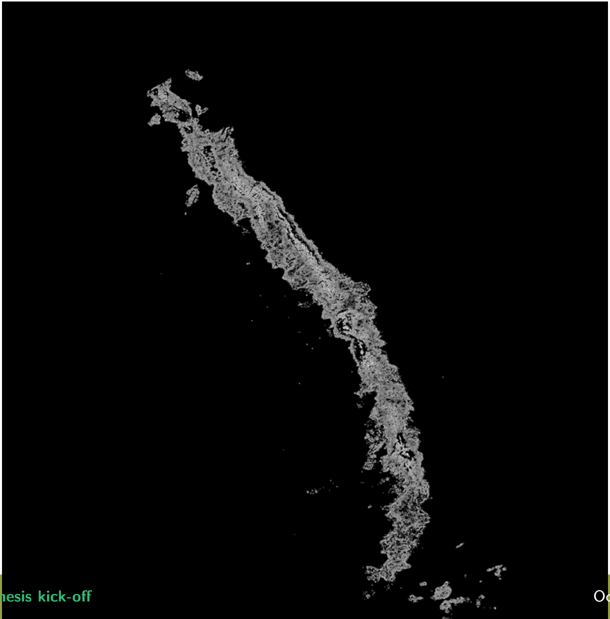

Musca $\mathcal{F}_{-0.1}$

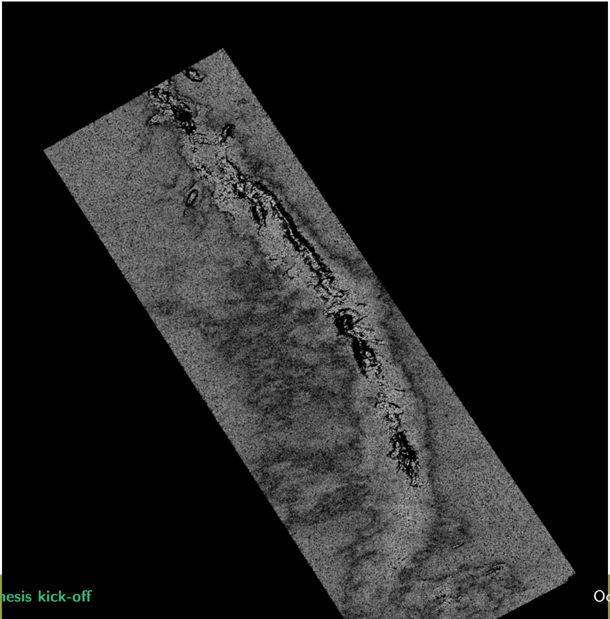

Musca $\mathcal{F}_0$

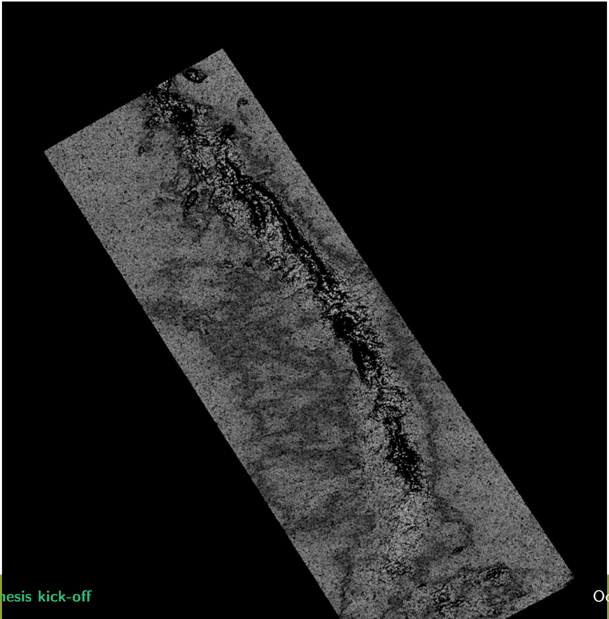

Musca $\mathcal{F}_0$ cut at 0

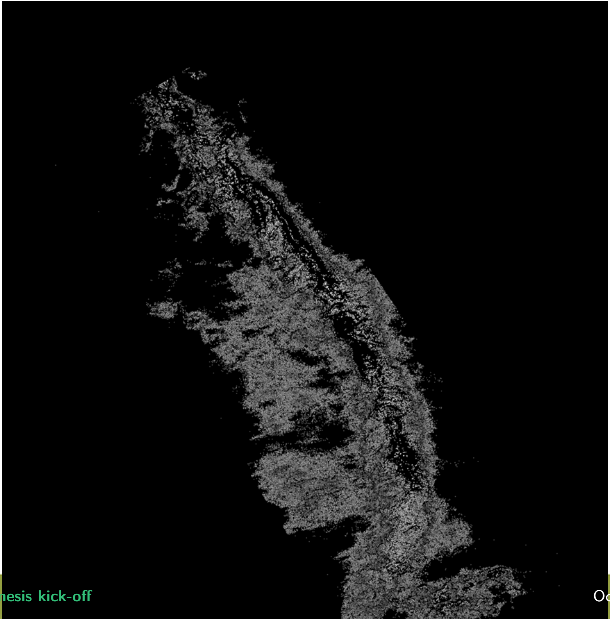

Musca $\mathcal{F}_{-0.4}$ spectrum

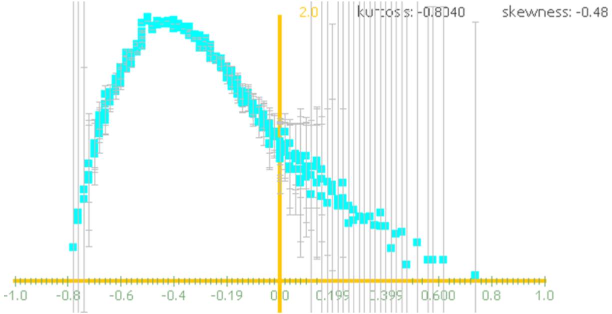

Musca $\mathcal{F}_{-0.3}$ spectrum

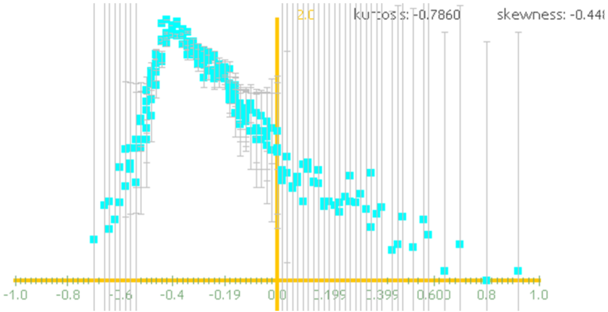

Musca $\mathcal{F}_{-0.2}$ spectrum

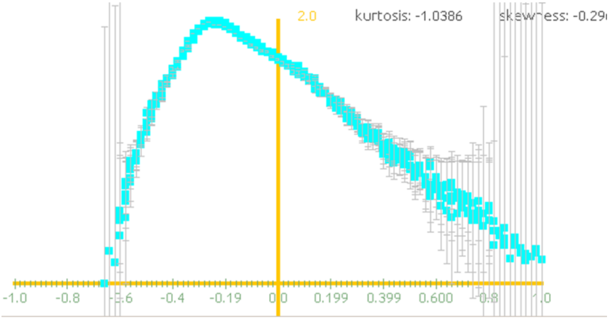

Musca $\mathcal{F}_{-0.2}$ spectrum, cut at 0

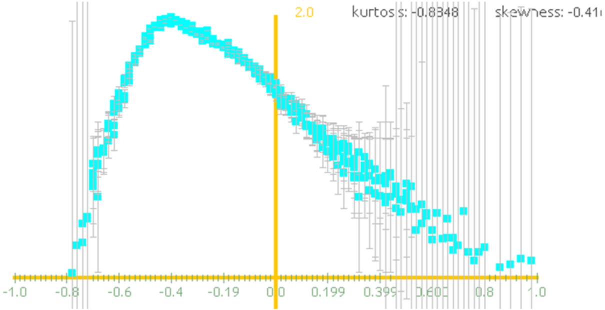

Musca $\mathcal{F}_{-0.1}$ spectum

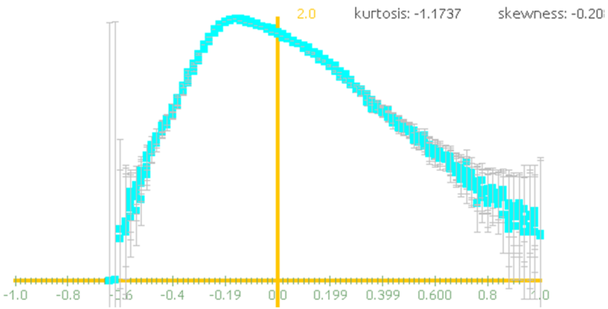

First conclusion

- These direct tools cannot distinguish between acquisisitions of a full 3D turbulent phenomenon.
- Still, they are consistent with the data and show properties.
- We must turn to more elaborate tools for analyzing cascading properties in 3D turbulence.
- Tests under way on the simulations provided by Nicola and Alexei.

4
Other approaches in computing spectra

Wavelet Transform Modulus Maxima

- Idea: use local maxima lines of wavelets coefficients to define a space-scale skeleton and follow crest lines.
-

Wavelet Transform Modulus Maxima

- Idea: use local maxima lines of wavelets coefficients to define a space-scale skeleton and follow crest lines.
- Let $\mathbf{s}$ be a signal, $\mathcal{T}_\psi(\mathbf{s}(\mathbf{x}), r) = \frac{1}{r^d} \int_{\mathbb{R}^d} \mathbf{s}(\mathbf{y}) \psi(\frac{\mathbf{x} - \mathbf{y}}{r}) d\mathbf{y}$, one has :$\mathcal{T}_\psi(\mathbf{s}(\mathbf{x}), r) \sim r^{\mathbf{h}(\mathbf{x})} \quad (r \to 0)$ si $\mathbf{s}(\mathbf{x})$ has $\mathbf{h}(\mathbf{x})$ as singularity exponent at $\mathbf{x}$.
-

Wavelet Transform Modulus Maxima

- Idea: use local maxima lines of wavelets coefficients to define a space-scale skeleton and follow crest lines.
- Let $\mathbf{s}$ be a signal, $\mathcal{T}_\psi(\mathbf{s}(\mathbf{x}), r) = \frac{1}{r^d} \int_{\mathbb{R}^d} \mathbf{s}(\mathbf{y})\psi(\frac{\mathbf{x}-\mathbf{y}}{r})d\mathbf{y}$, one has :$\mathcal{T}_\psi(\mathbf{s}(\mathbf{x}), r) \sim r^{\mathbf{h}(\mathbf{x})} \quad (r \to 0)$ si $\mathbf{s}(\mathbf{x})$ has $\mathbf{h}(\mathbf{x})$ as singularity exponent at $\mathbf{x}$.
- Partition function at order p and scale r:

$$Z(r, p) = \sum_{\alpha \in \mathcal{A}} |\mathcal{T}_\psi(\mathbf{s}(\mathbf{x}_\alpha(r)), r)|^p, \tag{28}$$

with $\mathcal{A}$ being the local maxima of $|\mathcal{T}_\psi(\mathbf{s}(\mathbf{x}), r)|$.

Wavelet Transform Modulus Maxima

- If the signal is multifractal and wavelet ψ correctly chosen, one has $Z(r,p) \sim r^{\tau_p}$.
-

Wavelet Transform Modulus Maxima

- If the signal is multifractal and wavelet ψ correctly chosen, one has $Z(r,p) \sim r^{\tau_p}$.
- Compute τ_p through regression then Legendre transform to get $D(\mathbf{h})$.

4
Singularity exponents computation in
microcanonical analogy

Relations with unpredictability

- If the physical signal **s** is multifractal, its singularity exponents are bounded. Define, as before the MSM (Most Singular Manifold):

$$\text{MSM} = \mathcal{F}_\infty = \{\mathbf{x} \mid \mathbf{h}(\mathbf{x}) \in]h_\infty - \Delta h, h_\infty + \Delta h[\}. \qquad (29)$$

-
-

Relations with unpredictability

- If the physical signal $\mathbf{s}$ is multifractal, its singularity exponents are bounded. Define, as before the MSM (Most Singular Manifold):

$$\mathrm{MSM} = \mathcal{F}_\infty = \{\mathbf{x} \mid \mathbf{h}(\mathbf{x}) \in]h_\infty - \Delta h, h_\infty + \Delta h[\}. \tag{30}$$

- Let $\nabla_\infty(\mathbf{s}) = \nabla_{\mathcal{F}_\infty}(\mathbf{s}) = \nabla_{|_{\mathcal{F}_\infty}} \mathbf{s} = \nabla \mathbf{s} \delta_{\mathcal{F}_\infty}$ be the current form associated to singular gradient.
-

Relations with unpredictability

- If the physical signal $\mathbf{s}$ is multifractal, its singularity exponents are bounded. Define, as before the MSM (Most Singular Manifold):

$$\mathrm{MSM} = \mathcal{F}_\infty = \{\mathbf{x} \mid \mathbf{h}(\mathbf{x}) \in]h_\infty - \Delta h, h_\infty + \Delta h[\}. \qquad (31)$$

- Let $\nabla_\infty(\mathbf{s}) = \nabla_{\mathcal{F}_\infty}(\mathbf{s}) = \nabla_{|\mathcal{F}_\infty}\mathbf{s} = \nabla\mathbf{s}\delta_{\mathcal{F}_\infty}$ be the current form associated to singular gradient.
- $\mathcal{F}_\infty$ = **most unpredictable manifold** $\Rightarrow$ one can reconstruct the whole signal from $\mathcal{F}_\infty$.

MSM

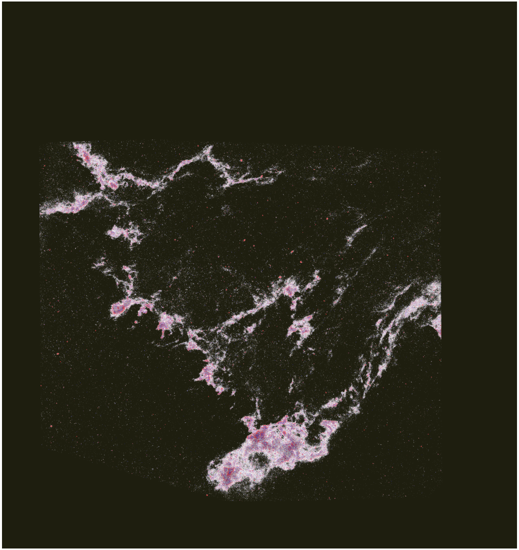

Figure: Draco: MSM + entropie.

Unpredictability and reconstruction

- So if $\mathcal{F}_\infty$ = **most unpredictable manifold** this implies we can reconstruct $\nabla \mathbf{s}(\mathbf{x}) = \mathcal{G}(\nabla_\infty(\mathbf{s}))(\mathbf{x})$.
-
-
-

Unpredictability and reconstruction

- So if $\mathcal{F}_\infty$ = **most unpredictable manifold** this implies we can reconstruct $\nabla \mathbf{s}(\mathbf{x}) = \mathcal{G}(\nabla_\infty(\mathbf{s}))(\mathbf{x})$.
- Physical hypothesis: $\mathcal{G}$ is linear and continuous: consequently it is an integral operator

$$\nabla \mathbf{s}(\mathbf{x}) = \int_{\mathcal{F}_\infty} \nabla \mathbf{s}(\mathbf{y}) G(\mathbf{x}, \mathbf{y}) d\mathbf{y}. \quad (35)$$

-
-

Unpredictability and reconstruction

- So if $\mathcal{F}_\infty$ = **most unpredictable manifold** this implies we can reconstruct $\nabla \mathbf{s}(\mathbf{x}) = \mathcal{G}(\nabla_\infty(\mathbf{s}))(\mathbf{x})$.
- Physical hypothesis: $\mathcal{G}$ is linear and continuous: consequently it is an integral operator

$$\nabla \mathbf{s}(\mathbf{x}) = \int_{\mathcal{F}_\infty} \nabla \mathbf{s}(\mathbf{y}) G(\mathbf{x}, \mathbf{y}) d\mathbf{y}. \tag{38}$$

- Physical hypothesis: trnaslational invariance $\Rightarrow$ convolution $\Rightarrow$ diffusion from $\mathcal{F}_\infty$:

$$\nabla \mathbf{s}(\mathbf{x}) = \int_{\mathcal{F}_\infty} \nabla \mathbf{s}(\mathbf{y}) G(\mathbf{x} - \mathbf{y}) d\mathbf{y}. \tag{39}$$

-

Unpredictability and reconstruction

- So if $\mathcal{F}_\infty$ = **most unpredictable manifold** this implies we can reconstruct $\nabla \mathbf{s}(\mathbf{x}) = \mathcal{G}(\nabla_\infty(\mathbf{s}))(\mathbf{x})$.
- Physical hypothesis: $\mathcal{G}$ is linear and continuous: consequently it is an integral operator

$$\nabla \mathbf{s}(\mathbf{x}) = \int_{\mathcal{F}_\infty} \nabla \mathbf{s}(\mathbf{y}) G(\mathbf{x}, \mathbf{y}) d\mathbf{y}. \tag{41}$$

- Physical hypothesis: trnaslational invariance $\Rightarrow$ convolution $\Rightarrow$ diffusion from $\mathcal{F}_\infty$:

$$\nabla \mathbf{s}(\mathbf{x}) = \int_{\mathcal{F}_\infty} \nabla \mathbf{s}(\mathbf{y}) G(\mathbf{x} - \mathbf{y}) d\mathbf{y}. \tag{42}$$

- One deduce:

$$\mathbf{s}(\mathbf{x}) = \int_{\mathcal{F}_\infty} \nabla \mathbf{s}(\mathbf{y}) \mathbf{g}(\mathbf{x} - \mathbf{y}) d\mathbf{y} \quad \text{for a propagation kernel } \mathbf{g}. \tag{43}$$

Unpredictability and reconstruction

- Fourier: $\hat{\mathbf{s}}(\mathbf{k}) = \hat{\mathbf{g}}(\mathbf{k})\widehat{\nabla_\infty}(\mathbf{s})(\mathbf{k})$.
-
-

Unpredictability and reconstruction

- Fourier: $\hat{\mathbf{s}}(\mathbf{k}) = \hat{\mathbf{g}}(\mathbf{k})\widehat{\nabla_\infty}(\mathbf{s})(\mathbf{k})$.
- To comply with power spectra properties, we consider the following propagator:

$$\hat{\mathbf{g}}(\mathbf{k}) = i\frac{\mathbf{k}}{\|\mathbf{k}\|^2}. \tag{46}$$

-

Unpredictability and reconstruction

- Fourier: $\hat{\mathbf{s}}(\mathbf{k}) = \hat{\mathbf{g}}(\mathbf{k})\widehat{\nabla_\infty}(\mathbf{s})(\mathbf{k})$.
- To comply with power spectra properties, we consider the following propagator:

$$\hat{\mathbf{g}}(\mathbf{k}) = i\frac{\mathbf{k}}{\|\mathbf{k}\|^2}. \tag{48}$$

- **Fundamental point:**

$$\operatorname{div}\left(\nabla_{\mathcal{F}_\infty}(\mathbf{s})\right) = 0. \tag{49}$$

Unpredictability and reconstruction

- Fourier: $\hat{\mathbf{s}}(\mathbf{k}) = \hat{\mathbf{g}}(\mathbf{k})\widehat{\nabla_\infty}(\mathbf{s})(\mathbf{k})$.
- To comply with power spectra properties, we consider the following propagator:

$$\hat{\mathbf{g}}(\mathbf{k}) = i\frac{\mathbf{k}}{\|\mathbf{k}\|^2}. \tag{50}$$

- **Fundamental point:**

$$\operatorname{div}\left(\nabla_{\mathcal{F}_\infty}(\mathbf{s})\right) = 0. \tag{51}$$

So the computation of exponents is local. But probably not the cascade properties !

h(x) computation

- Conséquence: **h**(**x**) is evaluated by a local impredictability measure:
-

$\mathbf{h}(\mathbf{x})$ computation

- Conséquence: $\mathbf{h}(\mathbf{x})$ is evaluated by a local impredictability measure:
- $$\mathbf{h}(\mathbf{x}) = \frac{\log(\mathcal{T}_\psi)(\mu)(\mathbf{x}, r_0))/\langle\mathcal{T}_\psi)(\mu)(\cdot, r_0)\rangle}{\log r_0} + o\left(\frac{1}{\log r_0}\right). \quad (53)$$

Developments

- Entropy.
- MHD.

Entropy

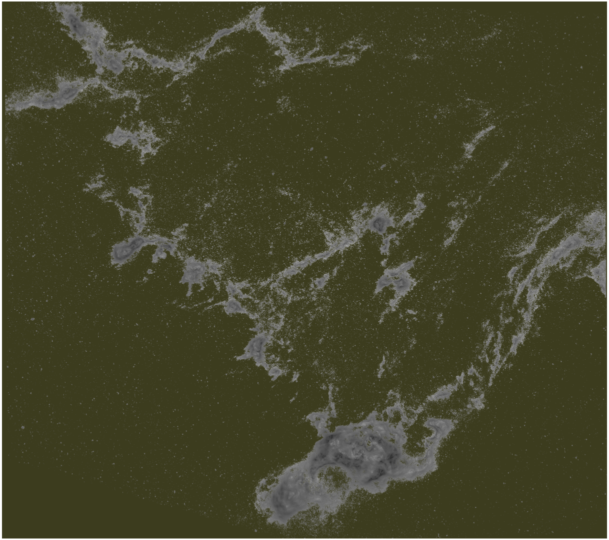

Figure: Modulus entropy derivative/unitary field.

Entropy

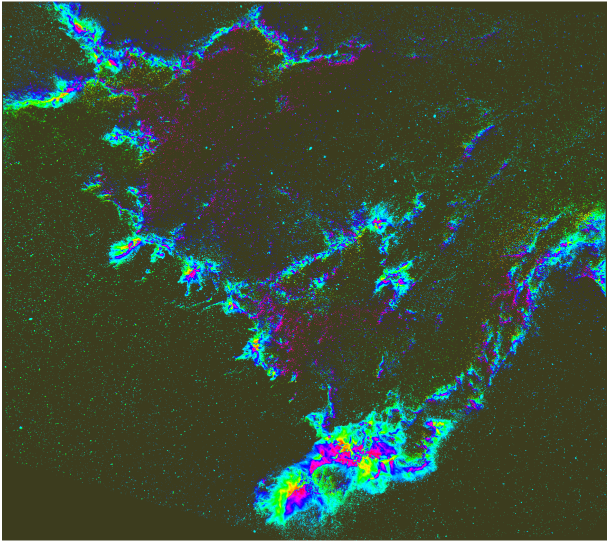

Figure: Phase entropy derivative/unitary field.

6
Conclusions

First conclusions

- Our techniques developed so far for remote sensing are not sufficient to analyze these fully 3D turbulent datasets.
- Multiplicative cascade analysis under WTMM formalism under way.
- It becomes apparent that the use of different kinds of data available will ease the analysis process.